Calorimetric Study of the Glassy State. XIII.* Thermodynamic Properties of Normal and Deuterated Orthoboric Acid Crystals

Masaharu OGUNI, Takasuke MATSUO, Hiroshi SUGA, and Syûzô SEKI
Department of Chemistry, Faculty of Science, Osaka University, Toyonaka, Osaka 560
(Received November 18, 1976)

Thermal properties of normal and deuterated orthoboric acids were studied through the measurements of heat capacity in the temperature range from 13 to 370 K by using an adiabatic calorimeter and differential thermal analysis curves above room temperature. For both crystals, the heat capacity anomaly was found around 290 K in the heat capacity values dependent upon the thermal history of the specimen; *i.e.*, the endothermic or exothermic enthalpy relaxation was observed in this temperature range. This behavior is of characteristic to the glass transition and is considered to be ascribed to the freezing-in phenomenon of the motion of rearrangement of the protons in hydrogen bondings. The enthalpy relaxation curves were analyzed with the exponential law and the characteristic time constant toward the equilibrium state was longer for enthalpy-excessive side than for enthalpy-deficient side. The glass transition temperature at which the endothermic relaxation time becomes 1 ks is 296.6 K for normal orthoboric acid and 298.2 K for deuterated orthoboric acid, respectively. The activation enthalpies were estimated to be 88 ± 5 and 91 ± 5 kJ mol^{-1} for the endothermic processes of normal and deuterated orthoboric acid, respectively. The melting points of normal and deuterated orthoboric acids were determined from the differential thermal analysis curves to be 169.9 and 167.4 °C, respectively.

Orthoboric acid crystal is a typical example of the hydrogen-bonded systems with two-dimensional structure being essentially a molecular arrangement of planar $B(OH)_3$ (see Fig. 10). Each hydroxyl group is linked by hydrogen bonds to two others belonging to different molecules and forms a six-membered hydrogen bonded ring. The hydrogen atom is situated on the O–O line, occupying the ordered position at room temperature.[1] The ring is arranged in a pattern of triangular lattice in two dimension and the crystal is built up by the superposition of these layers. There have been discussions about the position of the hydrogen atoms since the first determination of B and O positions by Zachariasen[2] in an early X-ray study. Electron diffraction study of the thin crystal by Cowley[3] showed that the hydrogen was displaced off the O–O bonds and that the hydrogen positions are disordered. The nonlinear O–H···O hydrogen model was also favored by Kume and Kakiuchi[4] in their NMR study, which was criticized in a subsequent recalculation by Ibers and Holm.[5] In the reinvestigation of the structure by X-ray method, Zachariasen[6] found the hydrogen atom situated on the O–O line. The neutron diffraction experiment,[1] designed specifically for the determination of the hydrogen position, seemed to have settled the discussion conclusively. In both X-ray and neutron diffraction studies it was also found that the layers are not strictly planar, but some tilts occur between the individually coplanar molecules.

However, two questions remain still open about the behavior of the hydrogen atom in the crystal. First, is the hydrogen position completely ordered at room temperature? The hydrogen bond length in orthoric acid is comparable with that in ice I_h for which existence of the hydrogen-positional disorder is well-established. Therefore, one may expect *partial* disordering of the hydrogen position in a double minimum potential of the hydrogen bonding in the present crystal, although complete disordering is ruled out by the neutron diffraction study.[1] If such a disorder was actually observed, one would find a very typical order-disorder transition in two dimensional system. Another question is how rapid would be the change of the hydrogen position in such an order-disorder system. Our experience with ice I_h,[7] heavy ice I_h,[8] $SnCl_2\cdot2H_2O$[9] and $SnCl_2\cdot2D_2O$[9] showed that the positional change of hydrogen atoms can be extremely slow in spite of the small mass of the atom at low temperature. Its relaxation time can be of the order of one minute or one hour, or for that matter, may be one year or one century. In such cases, we can observe the relaxation process calorimetrically as a glass transition phenomenon at some appropriate temperature.

In view of the current interest in the molecular relaxational phenomena in relatively simple substances, we have investigated orthoboric acid and its deuterated analog by low temperature heat capacity measurements, and in fact found heat capacity anomalies that possess every characteristic of a glass transition. Based on this observation of a glass transition, which implied the existence of partial disordering of hydrogen position, we performed differential thermal analysis (DTA) of the substance in the temperature region higher than the glass transition, for the purpose of investigating the behavior due to development of the hydrogen atom disordering with increasing temperature. This paper reports the experimental facts and their interpretation briefly.

Experimental

Preparation of the Material and the Heat Capacity Measurement. The heat capacity of normal (undeuterated) orthoboric acid crystal was measured for two different samples. The first sample, "Suprapur" reagent from Merck Co., was vacuum-dried for an hour at 20 °C in order to remove excess water if

* A part of this paper was presented on The Fourth International Conference of Chemical Thermodynamics, Montpéllier, 1975.

For part XII, see O. Haida, H. Suga, and S. Seki, *J. Chem. Thermodyn.*, in press.

any, and its heat capacity was measured in the temperature region between 13 and 315 K. The second was obtained by recrystallizing the extrapure grade reagent, purchased from Wako Pure Chemical Co., from the aqueous solution, and was investigated in the temperature region from 250 to 370 K. The deuterated orthoboric acid sample was obtained by recrystallization of B_2O_3 from heavy water solution (99.75%). The B_2O_3 crystals were prepared by complete dehydration of the normal orthoboric acid (purchased from Yamanaka Chemical Co.) by heating *in vacuo* to 200 °C for three days. The deuterium exchange ratio of the obtained crystals was analysed to be 99.5% by NMR method. The sample weight was 40.472, 48.586, and 53.495 g for the first and second samples of normal orthoboric acid and the deuterated orthoboric acid sample, respectively.

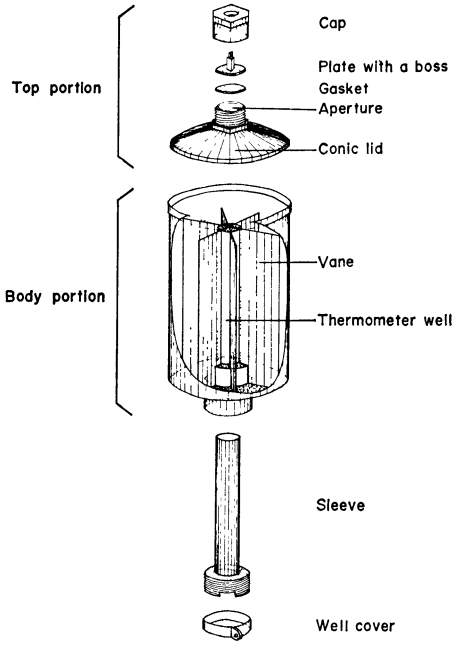

Fig. 1. A sectional drawing of the new calorimeter cell.

Calorimetric Apparatus. The calorimetric apparatus which was described before,[10] was so modified as to be capable of measurement up to 140 °C. Namely, the bronze adiabatic shields were replaced by those made of copper. This improved the temperature uniformity of the shields and hence the adiabatic regulation. The calorimeter cell, formerly sealed with low-melting solder, was replaced by a new cell of the Trowbridge and Westrum-type (marked with W-22) construction.[11] A sectional drawing of the cell pieces is given in Fig. 1. The body portion with a well and six vanes and the sleeve for a platinum thermometer were made of copper for achievement of rapid thermal equilibration, while the top portion, consisting of the cap, plate, and conic lid with an aperture, of stainless steel. The sleeve was settled on the body by being screwed in the well. High-melting solder was used for the seal between the lid and the body. The vacuum-tight closure was achieved by an annealed gold gasket forced against a circular knife edge of aperture. Plate with a boss served for preventing the gasket from turning in the closure by holding the boss. The typical equilibration time of the cell after turning off the calorimeter heater was around 13 min at room temperature. The second sample of the normal orthoboric acid and the deuterated orthoboric acid sample were measured with the improved apparatus. The inaccuracy of the measurement is estimated to be 1% at liquid hydrogen temperature and smaller than 0.2% above 40 K.

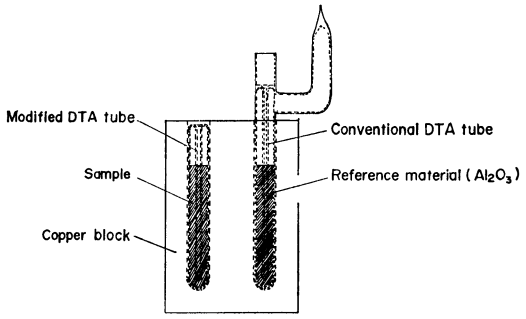

Fig. 2. Conventional and modified DTA tubes.

Differential Thermal Analysis. DTA studies of normal and deuterated orthoboric acids were carried out in the temperature region above the glass transition point. DTA apparatus previously reported[12] was modified for coping with the decomposition of the sample to metaboric acid and water vapor. For this purpose the sample tube as shown in Fig. 2 was used. The modified sample tube is smaller than the previous one. This modification decreased the dead volume in the tube and enabled the whole body of the sealed tube to be entirely embedded in the well of the copper block of the DTA apparatus. Thus any cold spot that might have caused trouble with the original sample tube was successfully avoided.

Results and Discussion

Melting. Melting of normal orthoboric acid has been reported by several authors. Carnelley[13] reported the melting at 184—186 °C from the heat capacity measurement and visual observation, and Stackelberg *et al.*[14] at 170 °C by visual observation under 4 atm pressure. Kracek *et al.*[15] obtained 170.9±0.2 °C from the solubility measurement. Benrath,[16] on the other hand, obtained 181 °C using the similar method. We performed the first observation for the melting of deuterated orthoboric acid, in addition to that of normal orthoboric acid. Figures 3 and 4 show melting curves in DTA for the normal and deuterated samples, respectively, obtained in the present study. The melting points were 169.9 and 167.4 °C for the respective substances, and the crystallization took place practically at the same temperature as the melting. These curves were reproduced repeatedly without significant changes.

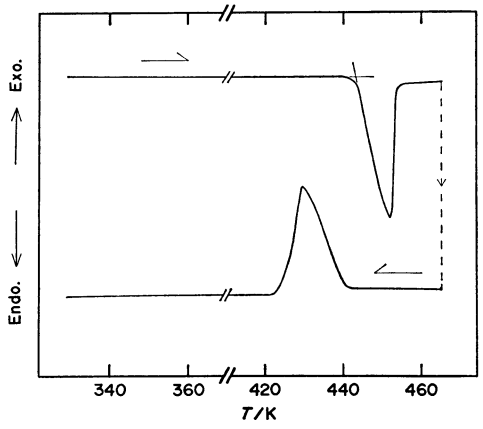

Fig. 3. DTA curves of normal orthoboric acid.

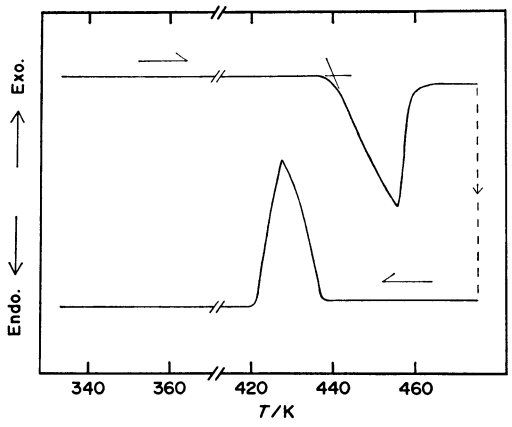

Fig. 4. DTA curves of deuterated orthoboric acid.

The melting points for normal orthoboric acid determined by Stackelberg *et al.* and Kracek *et al.* are in fairly good agreement with the present data, though their determination was performed through visual observation. The melting point of deuterated orthoboric acid is lower by 2.5 K than that of normal acid.

Heat Capacity. The heat capacity values are tabulated in Tables 1 and 2 for normal and deuterated orthoboric acid crystals, respectively. They are also shown in Fig. 5 as a function of temperature together with data (△) of Johnston and Kerr.[17] Johnston and Kerr's values are smaller than ours, the discrepancy increasing with the increasing temperature. This tendency may be attributed to a partial dehydration of their sample which might have happened during drying over a period of three days at 70 °C *in vacuo* in their

Table 1. Experimental molar heat capacity of normal orthoboric acid

T_{av}/K	C_p/J K^{-1} mol^{-1}	T_{av}/K	C_p/J K^{-1} mol^{-1}	T_{av}/K	C_p/J K^{-1} mol^{-1}	T_{av}/K	C_p/J K^{-1} mol^{-1}	T_{av}/K	C_p/J K^{-1} mol^{-1}
		58.29	22.35	165.44	51.47	300.69	86.73	291.95	80.76
First measurement		59.37	22.82	167.71	51.96	302.72	87.69	294.17	82.84
		60.48	23.31	170.03	52.48	304.72	88.23	296.27	84.79
		61.59	23.79	172.33	52.98	306.96	88.64	298.34	86.52
11.86	0.866	62.74	24.27	174.62	53.52	309.37	89.20	300.38	87.29
12.60	1.030	63.93	24.75	176.88	54.04	311.99	89.82	304.41	87.59
13.53	1.250	65.17	25.25	179.13	54.50			306.43	88.63
14.33	1.431	66.44	25.72	181.45	55.07	(annealed)		308.43	89.40
15.16	1.672	67.71	26.19	183.67	55.58			310.42	89.52
16.01	1.922	68.98	26.66	185.99	56.03	259.60	73.32	312.40	90.30
16.80	2.165	70.25	27.11	188.34	56.60	262.38	74.06		
17.60	2.432	71.52	27.57	190.82	57.20	264.94	74.59	(annealed)	
18.38	2.724	72.80	28.01	193.40	57.77	267.48	75.14		
19.16	3.018	74.09	28.45	195.96	58.38	270.01	75.78	262.13	73.95
19.93	3.318	75.36	28.90	198.50	58.97	272.52	76.33	264.46	74.50
20.70	3.646	76.63	29.32	201.02	59.53	275.01	77.05	266.78	75.05
21.50	3.993	77.91	29.76	203.60	60.12	277.58	77.65	269.11	75.57
22.32	4.346	79.16	30.18	206.24	60.79	280.19	79.04	271.41	76.09
23.13	4.746	80.43	30.59	208.86	61.40	282.74	80.24	273.70	76.73
20.86	3.741	75.10	28.79	211.45	61.98	285.21	81.71	276.02	77.27
21.71	4.091	77.62	29.64	214.08	62.57	287.64	83.36	278.32	77.94
22.67	4.546	79.79	30.37	216.69	63.18	290.05	84.88	280.57	78.81
23.73	4.997	81.90	31.07	219.23	63.75	292.43	86.10	282.94	80.31
24.72	5.487	83.97	31.73	221.83	64.39	294.79	86.86	285.42	81.95
25.65	5.923	85.99	32.37	224.50	65.02	297.13	87.10	287.81	83.57
26.55	6.393	88.08	33.00	227.14	65.66	299.46	87.41	290.13	84.94
27.47	6.833	90.22	33.58	229.76	66.29	301.80	87.46	292.41	86.08
28.35	7.281	92.33	34.15	232.37	66.93	304.12	87.97	294.69	86.54
29.19	7.727	94.51	34.73	235.00	67.53	306.43	88.38	296.97	86.86
30.00	8.179	96.76	35.31	237.65	68.18	308.74	88.96	299.24	87.26
30.81	8.595	98.98	35.89	240.29	68.85	311.03	89.60	301.57	87.44
31.66	9.069	101.16	36.43	243.86	69.53			303.95	87.98
32.53	9.520	103.32	36.93	246.44	70.18	Second measurement		306.30	88.39
33.38	9.998	105.44	37.58	249.00	70.77			308.65	89.06
34.19	10.43	107.55	37.91	250.87	71.27			312.89	90.09
35.02	10.88	109.66	38.54	253.70	71.89	(quenched)		315.44	90.78
35.88	11.35	111.84	39.07	256.32	72.54			318.21	91.50
36.76	11.83	114.11	39.62	259.02	73.19	241.09	68.99	320.96	92.41
37.65	12.32	116.34	40.15			243.50	69.45	323.69	92.95
38.56	12.77	118.55	40.69	(quenched)		245.90	70.05	326.40	93.76
39.47	13.25	120.73	41.21			248.29	70.62	329.10	94.50
40.38	13.72	122.98	41.73	260.38	73.45	250.67	71.14	331.78	95.25
41.27	14.19	125.22	42.23	262.96	74.02	253.02	71.72	334.44	96.07
42.12	14.60	127.43	42.78	265.30	74.59	255.36	72.28	337.09	96.60
42.95	15.05	129.62	43.28	267.43	74.97	257.68	72.84	339.72	97.40
43.76	15.46	131.79	43.78	269.54	75.61	258.04	72.86	342.42	98.20
44.54	15.84	133.94	44.29	271.65	76.14	260.34	73.47	345.21	98.95
45.37	16.26	136.12	44.78	273.76	76.66	262.64	74.02	347.97	99.72
46.28	16.73	138.34	45.28	275.86	77.15	264.93	74.60	350.82	100.55
47.26	17.15	140.53	45.78	277.96	77.60	267.21	75.09	353.74	101.26
48.09	17.62	142.77	46.28	280.06	78.03	269.48	75.65	356.64	102.07
49.07	18.12	145.05	46.81	282.15	78.50	271.74	76.54	359.53	102.86
50.08	18.59	147.30	47.31	284.26	78.94	274.00	76.76	362.40	103.69
51.10	19.08	149.53	47.88	286.37	79.50	276.27	77.13	365.25	104.40
52.12	19.56	151.81	48.33	288.47	79.91	278.53	77.67	368.07	105.15
53.14	20.02	154.13	48.87	290.56	80.41	280.79	78.35	370.88	105.89
54.14	20.49	156.40	49.38	292.62	80.89	283.05	78.71	373.68	106.68
55.16	20.95	158.71	49.91	294.66	81.78	285.31	79.33		
56.20	20.41	160.97	50.43	296.64	83.25	287.55	79.78		
57.24	21.88	163.21	50.89	298.65	85.29	289.76	80.47		

TABLE 2. EXPERIMENTAL MOLAR HEAT CAPACITY OF DEUTERATED ORTHOBORIC ACID

T_{av}/K	C_p/J K^{-1} mol^{-1}	T_{av}/K	C_p/J K^{-1} mol^{-1}	T_{av}/K	C_p/J K^{-1} mol^{-1}	T_{av}/K	C_p/J K^{-1} mol^{-1}	T_{av}/K	C_p/J K^{-1} mol^{-1}
12.66	1.044	82.35	31.93	178.62	60.02	325.87	103.95	304.15	98.26
15.48	1.828	84.30	32.60	180.95	60.68	328.62	104.76	306.44	98.84
17.10	2.366	86.20	33.19	183.26	61.49	331.44	105.63	308.73	99.25
18.54	2.900	88.16	33.82	185.55	62.19	334.25	106.36	311.02	99.52
19.89	3.445	90.18	34.42	187.83	62.52	337.03	107.13	313.30	100.27
21.15	3.976	92.17	35.04	190.10	63.30	339.79	108.11	315.57	100.98
22.25	4.494	94.11	35.63	192.33	64.11	342.54	108.66		
23.42	5.032	96.03	36.20	194.54	64.66	345.27	109.48	(annealed)	
24.67	5.643	97.97	36.79	182.89	61.39	347.98	110.34		
25.87	6.246	99.96	37.41	185.09	61.80	350.67	110.99	251.56	80.69
27.15	6.902	101.94	37.97	187.16	62.53	353.33	111.86	253.79	81.25
28.56	7.636	103.95	38.52	189.32	63.15	356.06	112.55	256.01	81.77
30.07	8.453	106.08	39.17	191.56	63.82	358.87	113.42	258.21	82.44
31.55	9.252	108.27	39.79	193.78	64.44	361.67	114.13	260.40	83.02
32.96	10.03	110.46	40.42	195.98	65.07	364.45	114.92	262.58	83.72
34.34	10.80	112.66	41.04	198.20	65.72	367.20	115.56	264.84	84.11
35.67	11.53	114.84	41.67	200.40	66.35	369.95	116.38	267.11	84.79
36.97	12.25	116.99	42.29	202.64	67.01	372.68	117.19	269.38	85.40
38.29	12.96	119.13	42.85	204.96	67.67			271.73	85.90
39.65	13.69	121.35	43.52	207.27	68.26	(quenched)		274.07	86.63
41.01	14.41	122.17	43.75	209.60	69.00			276.39	87.18
42.38	15.15	124.34	44.33	211.96	69.72	251.24	80.53	278.70	88.13
43.76	15.87	126.49	45.01	214.30	70.29	253.56	81.27	281.00	88.41
45.13	16.56	128.74	45.61	216.61	70.94	255.84	81.80	283.26	89.76
46.49	17.27	131.08	46.31	218.91	71.64	258.07	82.46	285.35	91.72
47.85	17.96	133.40	46.93	221.18	72.25	260.28	82.99	287.31	92.92
49.27	18.67	135.69	47.61	223.45	72.90	262.47	83.59	289.27	94.28
50.71	19.37	137.93	48.27	225.68	73.53	264.67	84.11	291.23	95.12
52.41	20.19	140.16	48.85	227.90	74.14	266.86	84.75	293.18	96.03
54.37	21.11	142.38	49.51	230.11	74.78	269.03	85.32	295.12	96.40
56.23	21.96	144.56	50.16	232.36	75.50	271.20	85.94	297.05	96.64
58.04	22.78	146.72	50.77	234.63	76.09	273.37	86.46	298.97	97.06
59.80	23.56	148.97	51.42	236.89	76.70	275.52	87.16	300.90	97.05
61.58	24.31	151.32	52.10	239.16	77.23	277.67	88.22	302.83	97.49
63.39	25.04	153.64	52.81	241.41	77.90	279.83	87.59	304.75	98.10
65.18	25.78	155.92	53.45	243.71	78.60	281.98	88.49	307.28	98.71
66.96	26.45	158.19	54.11	246.10	79.22	284.14	89.15	309.24	99.18
68.74	27.17	160.48	54.76	248.47	79.78	286.29	89.66	311.34	99.82
70.51	27.80	162.79	55.46	250.85	80.53	288.43	90.36	313.61	100.40
72.28	28.47	165.08	56.12			290.56	90.79		
74.06	29.11	167.35	56.76	313.43	100.19	292.66	91.40		
75.88	29.72	169.60	57.39	315.61	100.97	294.72	91.81		
77.72	30.37	171.82	58.07	317.92	101.56	296.94	93.83		
79.61	31.02	173.98	58.69	320.50	102.45	299.38	96.11		
80.37	31.29	176.25	59.25	323.20	103.24	301.79	97.42		

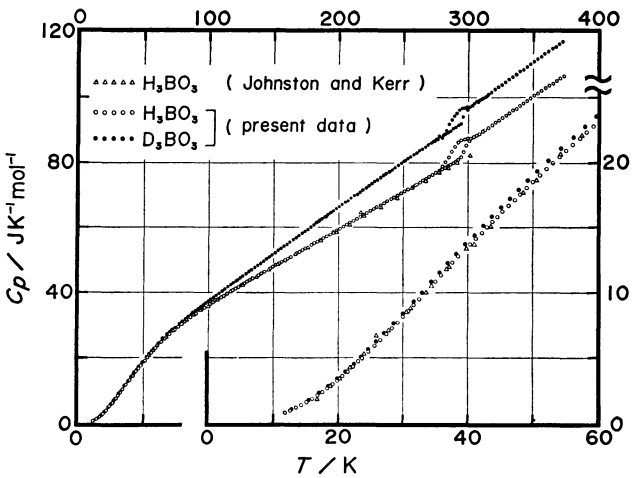

Fig. 5. Heat capacity of normal and deuterated orthoboric acids.

sample preparation. Johnston and Kerr stated that the heat capacity curve exhibits a double inflection at about 40 K. The anomaly is, however, scattering of their data. The present data, being more precise, preclude presence of any anomaly in this temperature region. Johnston and Kerr also mentioned the appearance of a spread-out hump, from about 20 to 150 K, which they interpreted as an indication of development of the hydrogen position disorder. However, this interpretation is not supported by recent evidence because the hydrogen atoms occupy almost completely their ordered positions even at room temperature, as was evidenced in a neutron diffraction study. It is likely that an unusual temperature dependence of the curve, resembling a spread-out hump, has the lattice-vibrational origin indicative of the two-dimensional feature of the crystal structure. Temperature dependence of the heat capacity of the deuterated orthoboric acid is similar to that of the normal acid, except that the deuterated compound has the larger heat capacity in the whole temperature range studied. Such an isotope effect is expected in terms of the increased mass by deuteration.

In contrast to the tolerably good agreement between the present data and those by Johnston and Kerr at the lower temperatures, there is a remarkable difference around 290 K. The present data exhibit occurrence of a step-like anomaly amounting to 3—4% of the total heat capacity. A similar anomaly is observed for the deuterat-

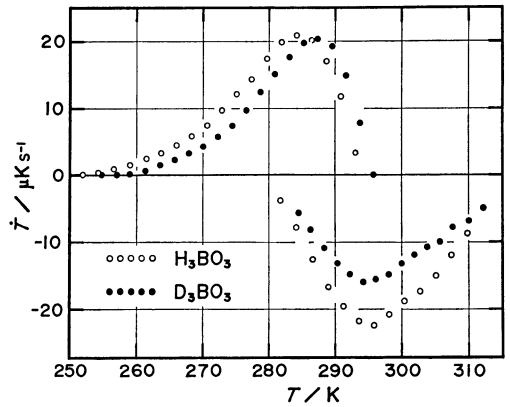

Fig. 6. Spontaneous temperature drift rate of the calorimeter cell for two different thermal treatments.

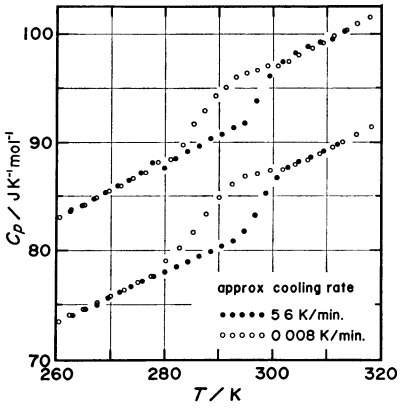

Fig. 7. Dependence of the heat capacity on the cooling rate around 290 K.

ed compound. A hysteretic behavior was also noted for both compounds at the same temperature. Thermal equilibration of the calorimeter was very sluggish in the temperature region between 260 and 310 K and an exothermic or endothermic effect was observed depending on the cooling rate and the thermal history of the sample. The heat capacity measurement was therefore performed in the following procedure. Prior to each measurement, the sample was first equilibrated at 315 K (at which temperature the thermal equilibrium was attained rapidly) and then cooled below 250 K at a respective cooling rate indicated in Fig. 7. A series of measurements was started at 250 K at which the temperature drift of the cell was normal within our experimental error. The temperature drift was then followed step by step up to 320 K. Each step of the measurement consisted of first heating the calorimeter by 2 K and then following its temperature drift. The energy input took 15 min and the drift measurement 40—60 min. Figure 6 illustrates the temperature drift rate of the calorimeter at 25 min after the calorimeter heater was switched off. If cooled rapidly the sample gave out heat in earlier stage of the subsequent warming, and then tended to absorb heat as indicated by the negative temperature drift at the higher temperature, whereas, if cooled slowly, it exhibited only negative temperature drift in the subsequent heat capacity measurement. The temperature drift approached normal behavior gradually above 300 K. This thermal behavior means that the anomaly in this region may be ascribed to a glass transition.[18] The heat capacity value was determined by employing the same method as used for $SnCl_2 \cdot 2H_2O$ and $SnCl_2 \cdot 2D_2O$.[9] The operational definition of the heat capacity involves an arbitrariness as to how the contribution from the strongly temperature-dependent relaxational degree of freedom is taken into account. The initial or final temperatures taken in the case of the exothermic drifts were calculated by extrapolating them to the mid-point of the heating period and consequently the contribution is excluded from the heat capacity, while in the endothermic case the temperatures at 40 min after the heating-off were employed as the temperatures for the heat capacity determination and therefore the heat capacities calculated involve the contribution deficiently or excessively compared with those in the equilibrium states. The heat capacity curve is illustrated in Fig. 7 in the temperature region from 260 to 320 K. The curve exhibits a clearly different behavior in the region depending on the cooling rate of the sample, *i.e.* the heat capacity is larger for the annealed sample than for the quenched one. This behavior can be also regarded as a general characteristic of a glass transition. The step-like increase around the transition point discloses the amount of configurational contribution to the heat capacity. The jump, ΔC_p, at 290 K was estimated by extrapolation to be 3.58 J K^{-1} mol^{-1} and 2.96 J K^{-1} mol^{-1} for the normal and deuterated orthoboric acids, respectively. It should be added that the behavior in the transition region was the same for the first and the second samples of normal orthoboric acid. This confirms that the glass transition is an intrinsic property of the substance.

Tables 3 and 4 give the thermodynamic functions derived from the smoothed heat capacity on the assumption that it jumps stepwise at 290 K. The heat capacity between 290 and 310 K where the annealing effect is prominent was estimated by extrapolation from above 310 K.

Kinetic Property of the Glass Transition. The exothermic and endothermic temperature drifts described above were analysed on the assumption that the

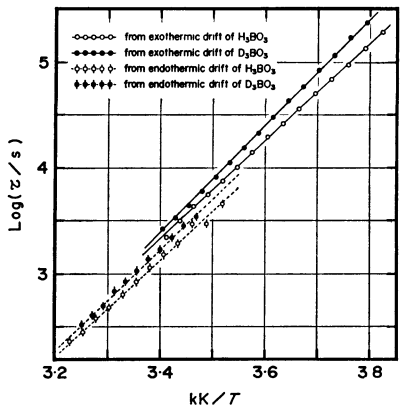

Fig. 8. Arrhenius plots of the characteristic times of exothermic and endothermic enthalpy relaxation drifts for normal and deuterated orthoboric acids.

Table 3. Thermodynamic functions of normal orthoboric acid

T/K	$C_p°$/J K^{-1} mol^{-1}	$S°-S_0°$[a)]/J K^{-1} mol^{-1}	$[H°-H_0°]/T$/J K^{-1} mol^{-1}
10	(0.54)	(0.185)	(0.138)
20	3.35	1.274	0.933
30	8.16	3.492	2.498
40	13.53	6.573	4.583
50	18.55	10.14	6.881
60	23.08	13.93	9.210
70	27.01	17.79	11.48
80	30.43	21.63	13.64
90	33.50	25.39	15.68
100	36.17	29.06	17.60
110	38.60	32.63	19.40
120	41.01	36.09	21.10
130	43.37	39.46	22.72
140	45.66	42.76	24.28
150	47.93	45.99	25.78
160	50.19	49.16	27.24
170	52.44	52.27	28.65
180	54.71	55.33	30.04
190	57.01	58.35	31.40
200	59.30	61.33	32.73
210	61.64	64.28	34.05
220	63.96	67.20	35.36
230	66.33	70.10	36.66
240	68.70	72.97	37.94
250	71.02	75.82	39.22
260	73.36	78.65	40.49
270	75.73	81.46	41.75
280	78.00	84.26	43.00
290	80.24	87.04	44.25
290	83.82	87.04	44.25
300	86.56	89.92	45.61
310	89.30	92.81	46.98
320	92.01	95.69	48.34
330	94.73	98.56	49.71
340	97.48	101.4	51.07
350	100.3	104.3	52.44
360	103.0	107.2	53.81
370	105.7	110.0	55.17
273.15	76.47	82.34	42.14
298.15	86.06	89.39	45.36
373.15	106.5	110.9	55.60

These thermodynamic functions were derived by assuming that the heat capacity jumps stepwise at 290 K. a) $S_0°$ is estimated to be 0.56 J K^{-1} mol^{-1} from molecular field approximation using heat capacity jump at 290 K.

Table 4. Thermodynamic functions of deuterated orthoboric acid

T/K	$C_p°$/J K^{-1} mol^{-1}	$S°-S_0°$[a)]/J K^{-1} mol^{-1}	$[H°-H_0°]/T$/J K^{-1} mol^{-1}
10	(0.54)	(0.184)	(0.138)
20	3.49	1.311	0.964
30	8.43	3.617	2.593
40	13.88	6.794	4.738
50	19.06	10.46	7.092
60	23.65	14.35	9.476
70	27.60	18.29	11.79
80	31.16	22.22	13.99
90	34.39	26.08	16.08
100	37.42	29.86	18.07
110	40.31	33.56	19.96
120	43.14	37.19	21.77
130	46.00	40.75	23.52
140	48.85	44.27	25.23
150	51.71	47.74	26.90
160	54.65	51.17	28.55
170	57.52	54.57	30.17
180	60.45	57.94	31.77
190	63.37	61.28	33.35
200	66.26	64.61	34.93
210	69.13	67.91	36.49
220	71.95	71.19	38.03
230	74.76	74.45	39.57
240	77.56	77.69	41.10
250	80.29	80.92	42.61
260	82.92	84.12	44.11
270	85.60	87.30	45.60
280	88.19	90.46	47.07
290	90.71	93.59	48.53
290	93.67	93.59	48.53
300	96.46	96.82	50.08
310	99.34	100.0	51.62
320	102.3	103.2	53.16
330	105.2	106.4	54.69
340	108.1	109.6	56.22
350	110.9	112.8	57.74
360	113.7	115.9	59.26
370	116.4	119.1	60.77
273.15	86.41	88.29	46.06
298.15	95.92	96.65	49.80
373.15	117.3	120.1	61.24

These thermodynamic functions were derived by assuming that the heat capacity jumps stepwise at 290 K. a) $S_0°$ is estimated to be 0.41 J K^{-1} mol^{-1} from molecular field approximation using heat capacity jump at 290 K.

enthalpy relaxation toward the equilibrium state follows an exponential law with a single relaxation time τ and they (*i.e.* exothermic and endothermic effects) were treated separately. The characteristic time for the former (*i.e.* exothermic) case was obtained by employing the evaluation method already explained in detail in the case of $SnCl_2 \cdot 2H_2O$ and $SnCl_2 \cdot 2D_2O$.[9] For the latter (*i.e.* endothermic) drift curves the exponential function fitted the experimental data within the imprecision of the temperature measurement, suggesting the validity of above assumption. The exothermic and endothermic effects resulted in two different straight lines as shown in Fig. 8, where the solid and dotted lines represent respectively the least square fits of the relaxation times derived from the exothermic and endothermic drifts. The difference means that the approach to the thermal equilibrium is governed by different characteristic times depending upon whether the equilibrium state is approached from the enthalpy-excessive side or from the enthalpy-deficient side. A similar behavior of the relaxation time was observed in $SnCl_2 \cdot 2H_2O$ and $SnCl_2 \cdot 2D_2O$. The Arrhenius plot of the relaxation

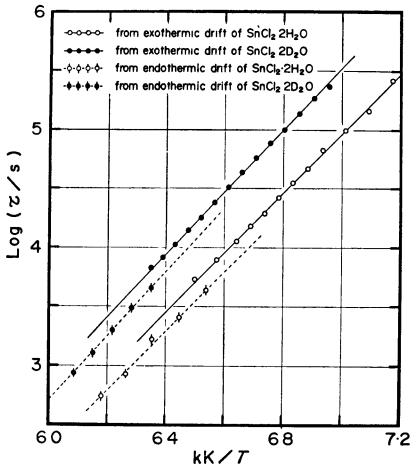

Fig. 9. Arrhenius plots of the characteristic times of exothermic and endothermic enthalpy relaxation drifts for $SnCl_2 \cdot 2H_2O$ and $SnCl_2 \cdot 2D_2O$.

time is shown in Fig. 9 for these compounds, where the relaxation times for the heat-absorption and heat-evolution processes follow different straight lines.

It should be noted that the characteristic time at a fixed temperature is longer for the exothermic process (*i.e.* on the enthalpy-excessive side) than for the endothermic process (*i.e.* on the enthalpy-deficient side) in these hydrogen-bonded systems. It should be added that the relaxation time was derived under the adiabatic condition. Thus, the temperature of the crystal changed as the relaxation proceeded. This means that the run of the adiabatic drift measurement corresponds to a small but finite temperature interval on the Arrhenius plot. This also means that the apparent final temperature to which the proton configuration tends is not constant but depends on the extent to which the relaxation has proceeded. These two aspects of the non-isothermal character of the drift measurement were not considered in the analysis of the relaxation effects in $SnCl_2 \cdot 2H_2O$ and $SnCl_2 \cdot 2D_2O$. Correction for these effects was found to decrease and increase the derived relaxation time typically by 0.5% for the exothermic and endothermic runs, respectively, and thus safely neglected. A relevant observation was reported by Davies and Jones[19] for glass transition in super-cooled liquids. They followed both the isothermal volume-relaxational change of glucose and the enthalpy-relaxational change of glycerol in the respective transition regions. According to their report, the characteristic time was longer on the volume-deficient (or enthalpy-deficient) side than on the volume-excessive (or enthalpy-excessive) side of the equilibrium state, and there occurred significant departure from the exponential form of the relaxation curve when the displacement from the equilibrium state was large. Thus the relaxational property of the present substance deviates from the idealized behavior, *i.e.* recovery of the equilibrium with a constant relaxation time independent of the sense and amount of the departure from the equilibrium. Furthermore, the deviation from the ideal relaxational behavior is in the direction opposite to Davies and Jones' observation on the super-cooled liquids. They explained their observation by arguing that the structure of the substance is looser in the volume-excessive state than in the volume-deficient state. Consequently the molecules are expected to be more mobile in the former non-equilibrium state, resulting in a smaller relaxation time. This is certainly a plausible explanation for the glassy liquids. In contrast, our present observation is difficult to understand in this intuitively agreeable argument. There exists, however, a peculiar character of the present hydrogen-boned system that might explain the difference qualitatively. In the glassy state of boric acid the hydrogen position has the long-range order, which means that if one particular site is occupied by a hydrogen atom an equivalent site in a distant unit cell has also non-zero probability of occupation by another hydrogen atom. When a disordered hydrogen atom tries to settle into a low energy site in the exothermic relaxation, it has a very limited choice as to the site it can occupy because the low energy site is dictated by the long-range order. In contrast, a molecule in a super-cooled liquid can find a local low energy conformation determined by its neighboring molecules. Thus, there is a formal probabilistic difference in addition to the structural and chemical differences between the long-ranged glassy state (glassy crystals) and the ordinary glassy state (glassy liquid). At present, however, we cannot find a convincing argument that relates the above mentioned peculiar features of the orthoboric acid with its observed relaxational property.

Table 5. Calorimetric quantities characterising the glass transition in H_3BO_3 and D_3BO_3 crystals

	T_g [a] / K	ΔC_p [b] / J K^{-1} mol^{-1}	σ [c]	$(H_a)_{exo}$ / kJ mol^{-1}	$(H_a)_{endo}$ / kJ mol^{-1}
H_3BO_3	296.6	3.58	0.94	89±5	88±5
D_3BO_3	298.2	2.96	0.96	97±5	91±5

a) The temperature at which the endothermic relaxation time becomes 1 ks. b) The heat capacity jump at 290 K in the transition region. c) The order parameter at 290 K estimated from the molecular field approximation.

The activation enthalpies estimated from the respective Arrhenius plots (Fig. 8) are given in Table 5 together with the glass transition points, the heat capacity jumps at 290 K, and the order parameters at 290 K calculated by a mean field approximation method. The values seem to be slighly larger for deuterated orthoboric acid than that for normal acid.

Interpretation of the Frozen-in Freedom. The glass transition in the present substance can be interpreted as the phenomenon originated from the disordered-frozen-in configuration of hydrogen-bonded system. Craven and Sabine[1] assigned uniquely all the atomic positions at room temperature. However the ordering of the atoms, in particular the hydrogen or deuterium atoms, is *not* completely attained in our interpretation. The six-membered oxygen ring, which is assumed to be the individual ordering unit of the hydrogen-bond network, has two permissible arrangements, *i.e.* clockwise and counterclockwise under the extended Bernal-Fowler condition, as is shown in Fig. 10. The interaction

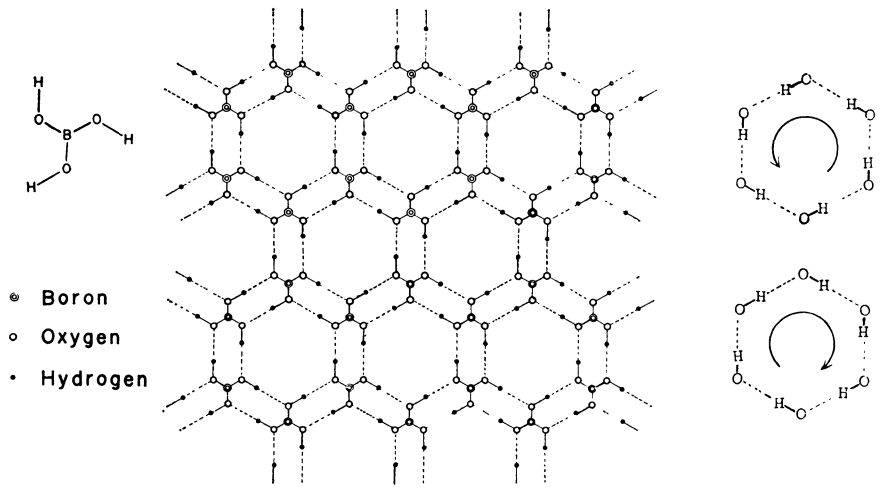

Fig. 10. The schematic atomic arrangement of a single layer in crystalline orthoboric acid and the two arrangements of the hydrogen atoms satisfying the local electric neutrality in the six-membered oxygen ring.

energy among the hydrogen-bonded hexagonal rings stabilizes the ferro-state where all of the hexagonal ring is the same (either all in the clockwise or all in the counterclockwise) arrangement. The entropy of this model is $(R/2)$ ln 2 at the completely disordered state. A mean field approximation can be applied, to a fairly good approximation, at the glass transition in such a system, since the hydrogen position is *almost* completely ordered at room temperature in the transition region. Then the order parameter σ is determined by the following equation at 290 K at which the configurational contribution to heat capacity is estimated:

$$C = \frac{\sigma R\left\{\ln\left(\frac{1+\sigma}{1-\sigma}\right)\right\}^2}{2\left\{\frac{2\sigma}{1-\sigma^2}-\ln\left(\frac{1+\sigma}{1-\sigma}\right)\right\}},$$

where the order parameter σ is given by $\sigma=(2n-N)/N$, n, the number of rearrangement units in the preferred arrangement, N, the number of total arrangement unit. The order parameter estimated at 290 K was *ca.* 0.94 and *ca.* 0.96 for normal and deuterated orthoboric acids, respectively. This degree of estimated ordering is consistent with Craven and Sabine's result[1] on account of the R factor in the neutron diffraction study. This interpretation of the "transition" as a relaxational effect of the hydrogen redistribution process in the crystal is also supported by comparison between the obtained activation energy and the hydrogen bond energy. The activation enthalpy of *ca.* 90 kJ mol^{-1} corresponds to the energy required for simultaneous activation of six hydrogen atoms, and therefore the activation enthalpy per atom amounts to *ca.* 15 kJ mol^{-1}, while the hydrogen bond energy between O–O in medium to long hydrogen bond systems such as ice is known to be 15—25 kJ mol^{-1}. These two values are in good agreement with each other, and thus the above interpretation of the transition would be reasonable provided that the activation process corresponds to the breaking of hydrogen bond.

There are alternative possibilities for the actual motion of the hydrogen atoms in the rearrangement. It is either an O–H librational mode around B–O axis or an O–H stretching-vibrational mode on an O–O bond. Recent NMR studies of inorganic hydrates have shown that a 180° flipping is a typical motion of water in the crystals.[20] If we adopted the former as the relevant mode, the activation enthalpy obtained above should be compared with the potential barrier (of the O–H librational mode) estimated by Durig *et al.*[21] They reported that the infrared absorption band at 808 cm^{-1} was assigned to this mode of vibration and estimated the potential barrier to be 96 kJ mol^{-1}. There is a large difference between this barrier height and the activation enthaply per hydrogen atom. The estimation of the hindering barrier rests entirely upon the assumption of a cosine-type potential function, which is not always a good approximation. In view of the hydrogen bond breaking of the mode discussed above, we may have to consider that the potential curve around the top of the barrier may be flatter than that given by the simple trigonometric function due to the interaction with the adjacent layer. A more reliable and direct estimation would be obtained by proton magnetic relaxation measurements. The relation between these two values will be a subject in the future work.

Deuterium Isotope Effect on a Glass Transition Temperature. In Table 6, the glass transition temperatures are collected for three hydrogen-bonded glassy crystals

TABLE 6. GLASS TRANSITION TEMPERATURE AND ITS DEUTERIUM ISOTOPE EFFECT FOR THREE HYDROGEN-BONDED GLASSY CRYSTALS

	T_g (H) / K	T_g (D) / K	T_g (D) − T_g (H) / K
$H_2(D_2)O$	107.6	126.1	18.5
$SnCl_2 \cdot 2H_2(D_2)O$	159.1	163.7	4.6
$H_3(D_3)BO_3$	296.6	298.2	1.6

The glass transition temperature is defined for ice as temperature at which the exothermic relaxation time becomes an hour, and for $SnCl_2 \cdot 2H_2O$ and H_3BO_3 as the temperature at which the endothermic relaxation time becomes 1 ks.

together with the corresponding data for the respective deuterium compounds. Here the glass transition temperature is defined as the temperature described below the table. Evidently, the isotope effect is larger in the substance with the lower glass transition temperature.

Further Discussion on the Absence of the Phase Transition. The hydrogen-bonding model illustrated in Fig. 10, and the interpretation of the glass transition deduced thereby, have a definite implication on the thermodynamics of the order-disorder system; the molar configurational entropy at infinite temperature is $(R/2)\ln 2$ and the heat capacity is equal to the jump in the observed heat capacity at the glass transition. These two quantities enable us to determine exactly the hypothetical transition temperature of the present hydrogen-bonded system by a statistical triangular Ising model;[22] 378 K for H_3BO_3 and 404 K for D_3BO_3. No phase transition is observed at these temperatures. The estimated transition temperature should be a lower limit because the lattice statistics involved is solved in two-dimensions. On the other hand, the upper limit is given by the molecular field approximation. The transition temperatures predicted by this approximation are 536 K and 587 K for the ordinary and the deuterated orthoboric acids, respectively. These temperatures are higher than the respective melting temperatures. We may conclude that we should have observed the transition if it was not interrupted by the melting. This may also imply that the interaction among the hexagonal rings is three-dimensional in spite of the structural two-dimensionality, because the absence of the phase transition below the fusion means that the hypothesized transition temperature lies much higher than the two-dimensional limit.

References

1) B. M. Craven and T. M. Sabine, *Acta Crystallogr.*, **20**, 214 (1966).
2) W. H. Zachariasen, *Z. Krist.*, **88**, 150 (1934).
3) J. M. Cowley, *Acta Crystallogr.*, **6**, 522 (1953).
4) K. Kume and Y. Kakiuchi, *J. Phys. Soc. Jpn.*, **15**, 1277 (1960).
5) J. A. Ibers and C. H. Holm, *J. Phys. Soc. Jpn.*, **16**, 839 (1961).
6) W. H. Zachariasen, *Acta Crystallogr.*, **7**, 305 (1954).
7) O. Haida, T. Matsuo, H. Suga, and S. Seki, *Proc. Jpn. Acad.*, **48**, 489 (1972); *J. Chem. Thermodyn.*, **6**, 815 (1974).
8) O. Haida, H. Suga, and S. Seki, *Proc. Jpn. Acad.*, **49**, 191 (1973).
9) T. Matsuo, M. Oguni, H. Suga, and S. Seki, *Proc. Jpn. Acad.*, **48**, 237 (1972); T. Matsuo, M. Oguni, H. Suga, S. Seki, and J. F. Nagle, *Bull. Chem. Soc. Jpn.*, **47**, 57 (1974).
10) T. Matsuo, H. Suga, and S. Seki, *J. Phys. Soc. Jpn.*, **30**, 785 (1971).
11) J. C. Trowbridge and E. F. Westrum, Jr., *J. Phys. Chem.*, **67**, 2381 (1963).
12) H. Suga, H. Chihara, and S. Seki, *Nippon Kagaku Zasshi*, **82**, 24 (1961).
13) T. Carnelley, *J. Chem. Soc.*, **18**, 273 (1878).
14) M. V. Stackelberg, F. Quantram, and J. Dressel, *Z. Elektroch.*, **43**, 14 (1937).
15) F. C. Kracek, G. W. Morey, and H. E. Merwin, *Am. J. Sci.*, **A35**, 143 (1938).
16) Von A. Benrath, *Z. Anorg. Chem.*, **249**, 245 (1942).
17) H. L. Johnston and E. C. Kerr, *J. Am. Chem. Soc.*, **72**, 4733 (1950).
18) H. Suga and S. Seki, *J. Non-Cryst. Solids*, **16**, 171 (1974).
19) R. O. Davies and G. O. Jones, *Adv. in Phys.*, **2**, 370 (1953).
20) H. Kiriyama, *Nippon Kessho Gakkai Shi*, **16**, 255 (1974).
21) J. R. Durig, W. H. Green, and A. L. Marton, *J. Mol. Struct.*, **2**, 19 (1968).
22) Private communication from Professor J. F. Nagle of the Carnegie-Mellon University to one (H. S.) of the present authors.